

# GLAUBER MODELING OF HIGH ENERGY HEAVY ION COLLISION

**Roli Esha**

*Semester 9*

*Under the guidance of*

**Dr. Bedangadas Mohanty**

National Institute of Science Education and Research

Bhubaneswar



November 15, 2012

## ACKNOWLEDGEMENTS

The desire to explore and scrutinize brings us closer to many alluring facts. I would like to extend my cordial gratitude to all the hands and minds behind the success of this project.

It is my privilege to thank my mentor, Dr. Bedangadas Mohanty for giving wings to the fire within and orienting to the world of high energy heavy ion collision physics. He was a constant source of inspiration and ever-generous with his knowledge. It was indeed a pleasure working with him.

I would also like to thank our group members for their help towards the successful completion of this venture.

In the end, I am grateful to my family and friends for their support.

~ Roli Esha

## ABSTRACT

We are using the Glauber Model to understand the initial conditions in heavy-ion collisions and the consequences on the particle production in these collisions. We have carried out as a part of the Masters thesis, both Optical and Monte Carlo Glauber model simulations to estimate initial magnetic field and angular momentum in heavy-ion collisions. In addition we have obtained initial geometrical features of the collisions as a function of impact parameter such as the number of participating nucleons, number of binary collisions, and eccentricity. Using the number of participating nucleons and binary collisions we are able to describe the charged particle multiplicity distributions in the high-energy heavy-ion collisions. The initial spatial eccentricity is found to be closely related to the experimentally measured momentum anisotropy. Finally we make a brief note on the effect of event-by-event fluctuations in the number of participating nucleons for a given impact parameter of the collision on multiplicity fluctuations measured in the experiments.

# Contents

<b>1</b>	<b>Introduction</b>	<b>1</b>
<b>2</b>	<b>Inputs to Glauber Model Calculations</b>	<b>4</b>
2.1	Nuclear charge density . . . . .	4
2.2	Inelastic nucleon – nucleon cross-section . . . . .	6
<b>3</b>	<b>Optical Glauber Model</b>	<b>8</b>
3.1	Formalism . . . . .	8
3.2	Coding the model . . . . .	10
3.3	Results and Discussion . . . . .	12
3.4	Computational methods . . . . .	16
<b>4</b>	<b>Monte Carlo Glauber Model</b>	<b>18</b>
4.1	Coding the model . . . . .	18
4.2	Results and Discussions . . . . .	19
<b>5</b>	<b>Relating Glauber Model to experiments</b>	<b>21</b>
5.1	Production of charged particles . . . . .	21
5.2	Eccentricity . . . . .	25
5.3	Angular momentum . . . . .	29
5.4	Electromagnetic field . . . . .	30
<b>6</b>	<b>Multiplicity fluctuations from Glauber Model</b>	<b>35</b>
<b>7</b>	<b>Summary and Conclusions</b>	<b>38</b>
	<b>References</b>	<b>41</b>
	<b>Appendix A Numerical integration techniques</b>	<b>43</b>
7.1	Trapezoidal integration . . . . .	43
7.2	Monte Carlo integration . . . . .	44
	<b>Appendix B Computing angular momentum</b>	<b>46</b>
	<b>Appendix C Computing magnetic field</b>	<b>47</b>
	<b>Appendix D Terminologies</b>	<b>49</b>

# Chapter 1

## Introduction

Developed by Roy Glauber (Nobel Prize in Physics, 2005) to address the problem of high energy scattering with composite particles, the Glauber model, provides a quantitative consideration of the geometrical configuration of the nuclei when they collide. It finds its basis in the concept of mean free path with minimal assumptions that the baryon – baryon interaction cross-section remains a constant throughout the passage of baryon of one nucleus into another and that the nuclei move along the collision direction in a straight line path. It is used to simulate the initial conditions in the heavy-ion collision and helps determine the number of participating nucleons in the particle production process and the number of binary collisions among the nucleons for the two nuclei, obeying a certain nuclear density distribution in a nucleus, colliding with a fixed energy for a given impact parameter. The Glauber model can be studied in two variants : the Optical approach and the Monte Carlo approach.

In the optical limit, the overall phase shift of the incoming wave is taken as a sum over all possible two nucleon phase shifts and the imaginary part of the phase shifts is related to the nucleon – nucleon scattering cross-section through the optical theorem<sup>1</sup>. A couple of assumptions are considered in the optical approximation as :

1. At sufficiently high energies, the nucleons carry sufficient momentum so as to pass undeflected through each other.

---

<sup>1</sup> The optical theorem is a general law of wave scattering theory, which relates the forward scattering amplitude to the total cross section of the scatterer. It is usually written in the form

$$\sigma_{\text{tot}} = \frac{4\pi}{k} \text{Im } f(0)$$

where  $f(0)$  is the scattering amplitude with an angle of zero, that is, the amplitude of the wave scattered to the center of a distant screen.

2. The nucleons move in the nucleus independently.
3. The size of the nucleus is much larger than the extent of the nucleon – nucleon force.

These hypotheses of linear independent trajectories of constituent nucleons make it plausible to develop an analytic relationship between the number of interacting nucleons and the number of nucleon – nucleon collisions in terms of basic nucleon – nucleon cross-section and the impact parameter of the nucleus – nucleus collision.

In the Monte Carlo ansatz of the Glauber model, a nucleus – nucleus collision is considered as a sequence of independent nucleon – nucleon collision processes. The Monte Carlo approach for determination of geometric quantities in the initial state of heavy ion collisions such as impact parameter, number of participating nucleons and number of binary collisions finds utmost utility in the simplicity of its implementation. This technique offers a closer simulation to the experimental conditions because of its following virtues :

1. The two colliding nuclei are assembled by positioning the nucleons randomly in a three-dimensional coordinate system, event-by-event, in accordance to the given nuclear density distribution.
2. Two nucleons are considered to collide if their distance,  $d$  in the plane orthogonal to the beam direction satisfies

$$d = \sqrt{\frac{\sigma_{inel}^{NN}}{\pi}} \quad (1.1)$$

where  $\sigma_{inel}^{NN}$  is the total inelastic nucleon – nucleon cross-section.

3. The number of participating nucleons and the number of binary collisions in a nuclear collision can be simply counted and averaged over multiple events.

In this report, both the ansatz of the Glauber model is discussed with emphasis on its development into the purely classical geometric picture used for present data analysis. In addition, the implications of the Glauber calculations of experimentally measurable quantities like number of charged particles produced, initial eccentricity, magnetic field and angular momentum and contribution of event-by-event number of participating nucleons towards measured multiplicity fluctuations is also discussed.

# Chapter 2

## Inputs to Glauber Model Calculations

In order to be able to compare the geometric results of this semi – classical model with the real experimental data, few model inputs are needed. The important ones among them are the nuclear density profile of the colliding nuclei and the energy dependence of the inelastic nucleon – nucleon cross–section.

### 2.1 Nuclear charge density

The Glauber model usually assumes the nucleon density inside the nucleus to be of the Woods – Saxon form

$$\rho(r) = \frac{\rho_0}{1 + e^{\frac{r-R}{a}}} \quad (2.1)$$

where  $R$  corresponds to the nuclear radius and  $a$  is a the diffusioness parameter that measures how quickly the nuclear density falls off at the surface of the nucleus.  $\rho_0$  is fixed by normalization condition. For a spherical nucleus,

$$\int \rho dV = \int_0^\infty 4\pi r^2 \rho(r) dr = A \quad (2.2)$$

where  $A$  is the number of nucleons (mass number) in the nucleus.

As an example, consider the hard sphere configuration.

$$\begin{aligned} \rho(r) &= \rho_0, r < R \\ &= 0, r \geq R \end{aligned} \quad (2.3)$$

In this case,

$$\rho_0 = \frac{A}{\frac{4}{3}\pi R^3} \quad (2.4)$$

which turns out to the order of 0.16 nucleon/fm<sup>3</sup> for gold nucleus ( $A = 197$ ), assuming  $R \sim R_0 A^{1/3}$  and  $R_0 \sim 1.12$  fm.

The actual value of the nuclear radius,  $R$ , can be empirically given in terms of  $A$  by the following empirical relation [5] :

$$R = 1.12 A^{1/3} - \frac{0.86}{A^{1/3}} \quad (2.5)$$

Though the functional form of  $\rho(r)$  is assumed to be of the Wood Saxon type, other more realistic forms derived from the electron scattering experiments can be used for a better insight. In case of some nuclei like Pb, the nucleon distribution has been obtained by scattering electrons off the nuclei. The density distribution is then parametrized and has the form [5]

$$\rho(r) = \frac{c_1 + c_2 r + c_3 r^2}{1 + e^{\left(\frac{r-R}{a}\right)}} \quad (2.6)$$

with  $R = 6.413$  fm and  $a = 0.5831$  fm and parameters

$$c_1 = 0.0633 \quad c_2 = -0.002045 \text{ fm}^{-1} \quad c_3 = 0.000566 \text{ fm}^{-2}$$

Most of the time the nuclei collided in experiments are symmetric, however deformed nuclei could provide additional physics insights. For example at the Relativistic Heavy Ion Collider Uranium ions are collided to understand the physics of Chiral Magnetic Effect (discussed later). For such deformed nuclei (<sup>238</sup>U) one uses a deformed Woods-Saxon profile [6]

$$\rho(r) = \frac{\rho_0}{1 + e^{\left(\frac{r-R'}{a}\right)}} \quad (2.7)$$

where  $\rho_0$  is the normal nuclear density and  $R'$  is expressed in terms of spherical harmonics and set of deformation parameters as

$$R' = R [1 + \beta_2 Y_2^0(\theta) + \beta_4 Y_4^0(\theta)] \quad (2.8)$$

Here  $R = 6.81$  fm is the mean radius of the nucleus and  $a = 0.55$  fm is the diffuseness parameter.  $Y_l^m(\theta)$  denote the spherical harmonics and  $\theta$  is the polar angle with respect to the symmetry axis of the nucleus. The deformation parameters are  $\beta_2 = 0.28$  and  $\beta_4 = 0.093$  for  $^{238}\text{U}$ .

## 2.2 Inelastic nucleon – nucleon cross-section

The Glauber model assumes that the nucleons collide inelastically and the number of charged particles produced on each collision to remain the same on an average. As the energy loss and change in momentum in each collision is small, multiple collisions can occur with same cross-section. This static cross-section is assumed to be the same as that for a single proton – proton collision and does not depend on the nuclear environment. In addition, interchangeability of protons and neutrons is inherent to the model.

As the cross-section involves processes with low momentum transfer, we cannot employ perturbative QCD calculations as these are found to be valid for transverse momentum,  $p_T \geq 1$  GeV/c [7] [8]. Hence, experimentally measured values of inelastic nucleon – nucleon cross-section ( $\sigma_{inel}^{NN}$ ) is used as input. This provides for the only non-trivial dependence of the Glauber calculation on the beam energy,  $\sqrt{s}$ .

The values of inelastic nucleon – nucleon cross-section for some characteristic beam energies are summarized in Table 2.1.

Table 2.1: Experimental values for  $\sigma_{inel}^{NN}$  for given beam energy

$\sqrt{s}$ (GeV)	$\sigma_{inel}^{NN}$ (mb)	$\sigma_{inel}^{NN}$ ( $fm^2$ )	Reference
7.7	30.8	3.08	[9]
11.5	29.73	2.973	[9]
17.2	29.5	2.95	[9]
19.6	30.08	3.008	[9]
27	31.94	3.194	[9]
39	30.98	3.098	[9]
62.4	31.55	3.155	[9]
200	42	4.2	[10]
2760	64	6.4	[10]
5500	72	7.2	[11]

# Chapter 3

## Optical Glauber Model

In the Optical Glauber model calculations, the nucleus is assumed to comprise of smooth matter density described by Fermi distribution in radial direction and uniform over the polar and azimuthal angles.

### 3.1 Formalism

Impact vector is given by the line joining the centers of the two colliding nuclei in the plane perpendicular to the beam direction. The length of the impact vector is called the impact parameter ( $b$ ). Small impact parameter collisions are called central collisions while large impact parameter collisions are called peripheral collisions. Consider two heavy ions, target (A) and projectile (B) colliding at relativistic speed with an impact parameter ( $b$ ) as shown in Fig. 3.1.

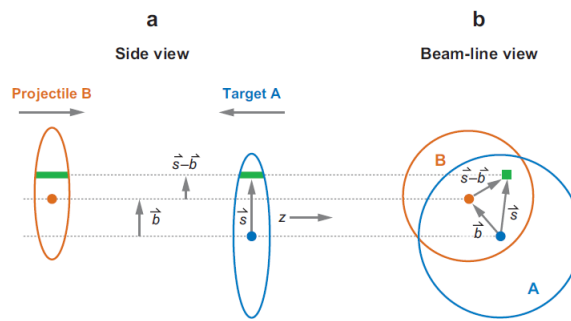


Figure 3.1: Schematic representation of Optical Glauber model geometry.

We will concentrate in the region of the two flux tubes which are located at a displacement  $\mathbf{s}$  from the center of the target nucleus and  $\mathbf{s} - \mathbf{b}$  from the center of the

projectile nucleus. During the collision, these two tubes overlap. The length of the tube depends upon its distance from the center of the nuclei. The probability per unit transverse area of a nucleon being located in the flux tube is given by the nuclear thickness function, defined as,

$$T_{A/B}(\mathbf{b}) = \int \rho_{A/B}(\mathbf{b}, z_{A/B}) dz_{A/B} \quad (3.1)$$

where  $\rho_{A/B}(\mathbf{b}, z_{A/B})$  is the probability of finding a nucleon at a point  $(\mathbf{s}, z_{A/B})$  per unit volume in projectile (A) or target (B) nucleus, normalized to unity. This information is obtained through nuclear density profile of the respective colliding nuclei. Thus, the joint probability per unit area of finding nucleons in the respective overlapping region will be given by what is defined as the **thickness function**.

$$T_{AB}(\mathbf{b}) = \int T_A(\mathbf{s}) T_B(\mathbf{s} - \mathbf{b}) d^2s \quad (3.2)$$

The integral over all impact parameter for  $T_{AB}$  is given by

$$\int T_{AB}(\mathbf{b}) d\mathbf{b} = A \cdot B \quad (3.3)$$

Since  $T_{AB}(\mathbf{b})$  is purely a geometric factor, it is independent of the collision energy. The number of inelastic nucleon – nucleon collision as a function of the impact parameter is given as

$$N_{coll}(\mathbf{b}) = \sigma_{inel}^{NN} T_{AB}(\mathbf{b}) \quad (3.4)$$

$N_{coll}$  depends on the beam energy through  $\sigma_{inel}^{NN}$ .

The probability of  $n$  inelastic NN collisions at an impact parameter  $\mathbf{b}$  is given by

$$P(n, \mathbf{b}) = {}^{AB}C_n \left[ \frac{\sigma_{inel}^{NN} T_{AB}(\mathbf{b})}{AB} \right]^n \left[ 1 - \frac{\sigma_{inel}^{NN} T_{AB}(\mathbf{b})}{AB} \right]^{AB-n} \quad (3.5)$$

The number of participants in nucleus – nucleus collision can be obtained from a hadron – nucleon collision. So, setting  $B = 1$ , the probability, thus, becomes

$$P(n, \mathbf{b}) = {}^AC_n \left[ \frac{\sigma_{inel}^{NN} T_A(\mathbf{b})}{A} \right]^n \left[ 1 - \frac{\sigma_{inel}^{NN} T_A(\mathbf{b})}{A} \right]^{A-n} \quad (3.6)$$

Summing over all probabilities, we obtain,

$$\sum_{n=1}^A P(n, \mathbf{b}) = 1 - \left[ 1 - \frac{\sigma_{inel}^{NN} T_A(\mathbf{b})}{A} \right]^A \quad (3.7)$$

If  $\sigma_{inel}^{NN} T_A(\mathbf{b})/A \ll 1$  then the above sum can be approximated by exponential so that

$$\sum_{n=1}^A P(n, \mathbf{b}) = 1 - \exp[-\sigma_{inel}^{NN} T_A(\mathbf{b})] \quad (3.8)$$

The number of participants in nucleus A is proportional to the nuclear profile function at transverse position  $\mathbf{s}$ ,  $T_A(\mathbf{s})$ , weighted by the sum over the probability for a nucleon-nucleus collision at transverse position  $(\mathbf{b} - \mathbf{s})$  in nucleus B. Thus at a given  $\mathbf{b}$ , the number of participants is given by

$$\begin{aligned} N_{part}(\mathbf{b}) &= \int T_A(\mathbf{s}) (1 - \exp[-\sigma_{inel}^{NN} T_B(\mathbf{b} - \mathbf{s})]) ds \\ &+ \int T_B(\mathbf{b} - \mathbf{s}) (1 - \exp[-\sigma_{inel}^{NN} T_A(\mathbf{b})]) ds \end{aligned} \quad (3.9)$$

## 3.2 Coding the model

The following algorithm was employed to get the dependence of the number of participating nucleons and the number of binary nucleon – nucleon collision as a function of impact parameter for a given nuclear density profile and inelastic nucleon – nucleon cross-section.

- The functional form of the density profile,  $\rho(r)$  is given as input. The functional dependence of mean nuclear radius,  $R$  on number of nucleons in the nucleus,  $A$  is specified. The value of skin depth,  $a$  is put in. These informations are used to get the normalization,  $\rho_0$  using

$$\rho_0 = \frac{A}{4\pi t}$$

where  $t = \int_0^\infty r^2 \rho(r) dr$  for a spherical nucleus. The nuclear density function hence becomes  $\rho_0 \rho(r)$ .

- The thickness function is computed using

$$T(x, y) = \int \rho_0 \rho(x, y, z) dz$$

where  $r = \sqrt{x^2 + y^2 + z^2}$

- Various observables are then computed in terms of the impact parameter,  $b$  as

$$T(b) = \int \rho_0 \rho(x + b, y, z) dx dy dz = \int T(x + b, y) dx dy \quad (3.10)$$

$$\begin{aligned} T_{AB}(b) &= \int \rho_0^2 \rho(x + b, y, z) \rho(x, y, z) dx dy dz \\ &= \int T(x + b, y) T(x, y) dx dy \end{aligned} \quad (3.11)$$

$$N_{coll}(b) = \sigma_{inel}^{NN} T_{AB}(b) \quad (3.12)$$

$$\begin{aligned} N_{part}(b) &= \int T(x, y) (1 - e^{-\sigma_{inel}^{NN} T(x+b, y)}) dx dy \\ &+ \int T(x + b, y) (1 - e^{-\sigma_{inel}^{NN} T(x, y)}) dx dy \end{aligned} \quad (3.13)$$

The details are discussed in the appendix.

### 3.3 Results and Discussion

The model is applied to the Lead ( $^{208}\text{Pb}$ ) nuclei (Pb–on–Pb collision) in order to get the number of participants and number of binary nucleon – nucleon collisions as a function of impact parameter. Various density profiles, as shown in Fig. 3.2, are used so as to get a better insight into the model.

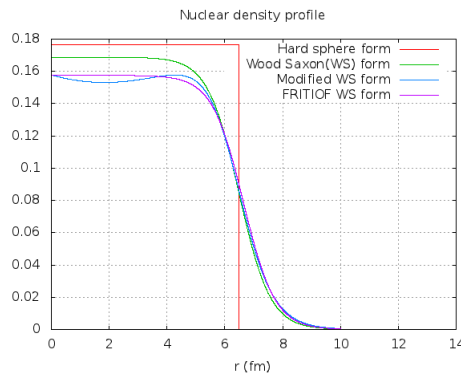


Figure 3.2: Various nuclear density profiles used for calculations for Lead (Pb) nuclei.

The nuclear density functions used are given in Table 3.1.

Using the  $\sigma_{inel}^{NN} = 31.5$  mb, which averages the cross-section for inelastic interaction within the center of mass energy range of 7 to 60 GeV, further estimates for dependence of number of participants and number of binary collisions on impact parameter were made as shown in Fig. 3.3. Smaller impact parameter in a geometrical picture implies larger overlap, usually termed as central collisions and larger impact parameter collisions have smaller overlap region and termed as peripheral collisions. Hence the number of participating nucleons and number of binary collisions decreases with increase in the impact parameter values.

Table 3.1: Nuclear density functions used for calculation for Lead (Pb) nuclei.

Name	$\rho(r)$ (fm <sup>-3</sup> )	R (fm)	a (fm)	Ref.
Hard sphere	$\rho(r) = \rho_0$ if $r \leq R$ $= 0$ otherwise	$1.16A^{1/3} - 0.86A^{-1/3}$	0.54	
Wood Saxon	$\rho(r) = \frac{1}{1+e^{\left(\frac{r-R}{a}\right)}}$	$1.16A^{1/3} - 0.86A^{-1/3}$	0.54	
Modified Wood Saxon	$\rho(r) = \frac{c_1+c_2r+c_3r^2}{1+e^{\left(\frac{r-R}{a}\right)}}$ $c_1 = 0.0633$ $c_2 = -0.002045 \text{ fm}^{-1}$ $c_3 = 0.000566 \text{ fm}^{-2}$	6.413	0.5831	[5]
FRITIOF Wood Saxon	$\rho(r) = \frac{1}{1+e^{\left(\frac{r-R}{a}\right)}}$	$1.16(A^{1/3} - 1.16A^{-1/3})$	0.545	[5]

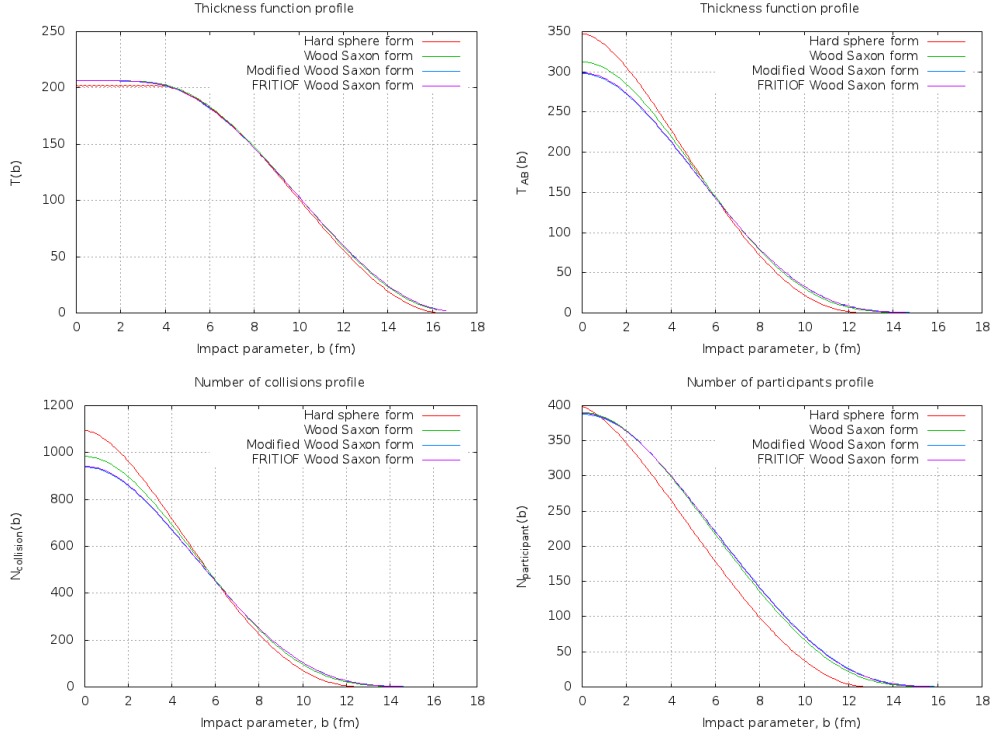


Figure 3.3: Nuclear thickness functions, Number of binary collisions and Number of participating nucleons as a function of impact parameter for Pb-Pb collisions at  $\sqrt{s_{NN}} = 11.5$  GeV.

The mean radius of a nucleus,  $R$ , scale as  $A^{1/3}$ , where  $A$  is the mass number. Hence, the geometric hadronic cross-section,  $\sigma_{AA}$ , between two similar nuclei will scale as  $A^{2/3}$ . Number of participants,  $N_{part}$ , scales as  $A$ . For hard processes that scale as number of binary collisions,  $N_{coll}$ , we use the binary scaling hypothesis for hard processes (details in the next chapter). Let the hard cross-section be  $d\sigma$  and total cross-section be  $\sigma$ . For two colliding nuclei with mass numbers  $A$  and  $B$  respectively, the differential cross-section,  $d\sigma_{AB}$ , is given by

$$d\sigma_{AB} = A \cdot B \cdot d\sigma_{NN} \quad (3.14)$$

Thus, we have

$$1 = \frac{d\sigma_{AB}/\sigma_{AB}}{(N_{coll}/\sigma_{pp})/d\sigma_{pp}} \sim \frac{(A^2/A^{2/3})}{N_{coll}} \quad (3.15)$$

This gives that  $N_{coll}$  scales as  $A^{4/3}$  for similar target and projectile nuclei.

Hence, from geometric considerations it is estimated that

$$N_{coll} \propto N_{part}^x$$

This was tested for the various density profiles used and the value of  $x$  was determined in each case. The plots for  $N_{coll}$  versus  $N_{part}$  is given in Fig. 3.4.

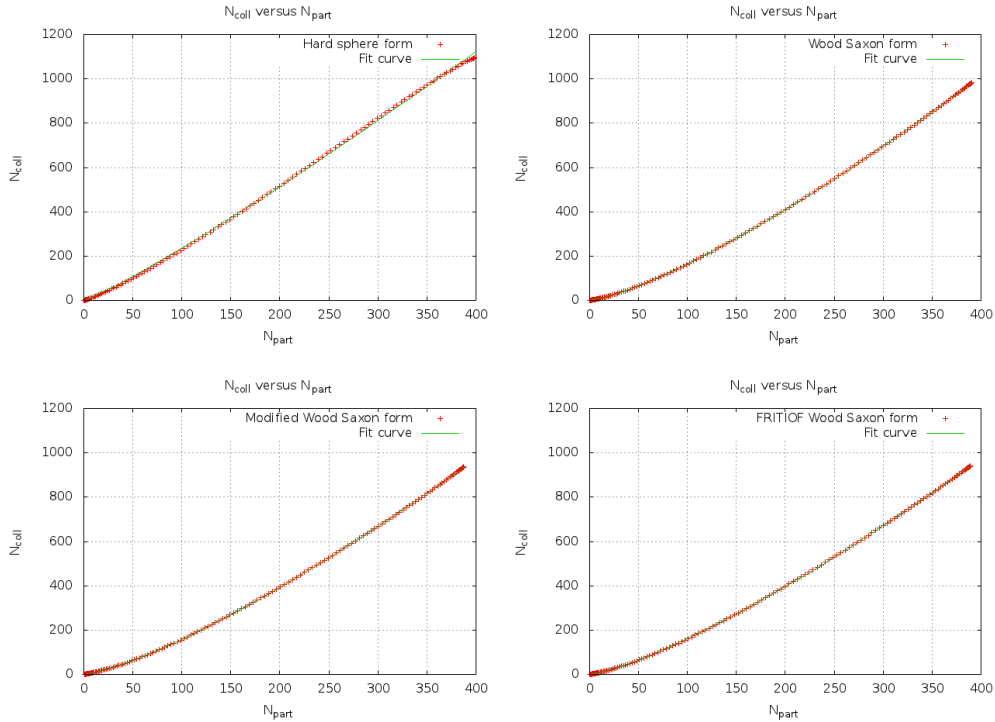


Figure 3.4:  $N_{coll}$  versus  $N_{part}$  for various density profiles for Pb-Pb collisions at  $\sqrt{s_{NN}} = 11.5$  GeV.

For the hard sphere form, the value of  $x$  was determined to be 1.12753, while for the Woods – Saxon form, it was 1.31006. For the Modified Wood Saxon form, the value of  $x$  was found to be 1.30992 and 1.29727 for the FRITIOF Wood Saxon

form of nuclear density function. This is in accordance with the theoretical value of  $x = 4/3$ .

The scaling of  $N_{part}$  with the number of nucleons in the colliding nuclei starts to saturate with increase in atomic number (Fig. 3.5).

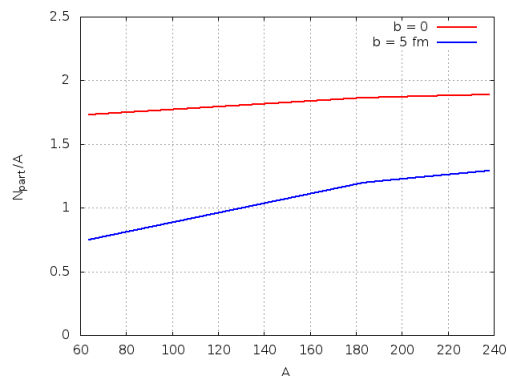


Figure 3.5: Scaling of  $N_{part}$  with  $A$ .

It may be noted that quantities like impact parameter, number of participating nucleons and number of binary collisions are not all directly measurable in experiments, while they are very important quantities from theoretical perspective. Glauber model provides a way to make the connection between theoretically calculated quantities and experimentally measured observables. This is discussed later on in the report.

### 3.4 Computational methods

In order to carry out the integrations required (Equations 3.10–3.13) in the Optical Glauber model to estimate the number of nucleons participating in the particle production process and the number of binary collisions between the nucleons during nucleus – nucleus collision, different numerical integration techniques are used, namely, the trapezoidal integration and the Monte Carlo integration methods. The

details of the program is given in the appendix with a very brief description of the techniques used.

Comparison of results from the two techniques is shown in Fig. 3.6.

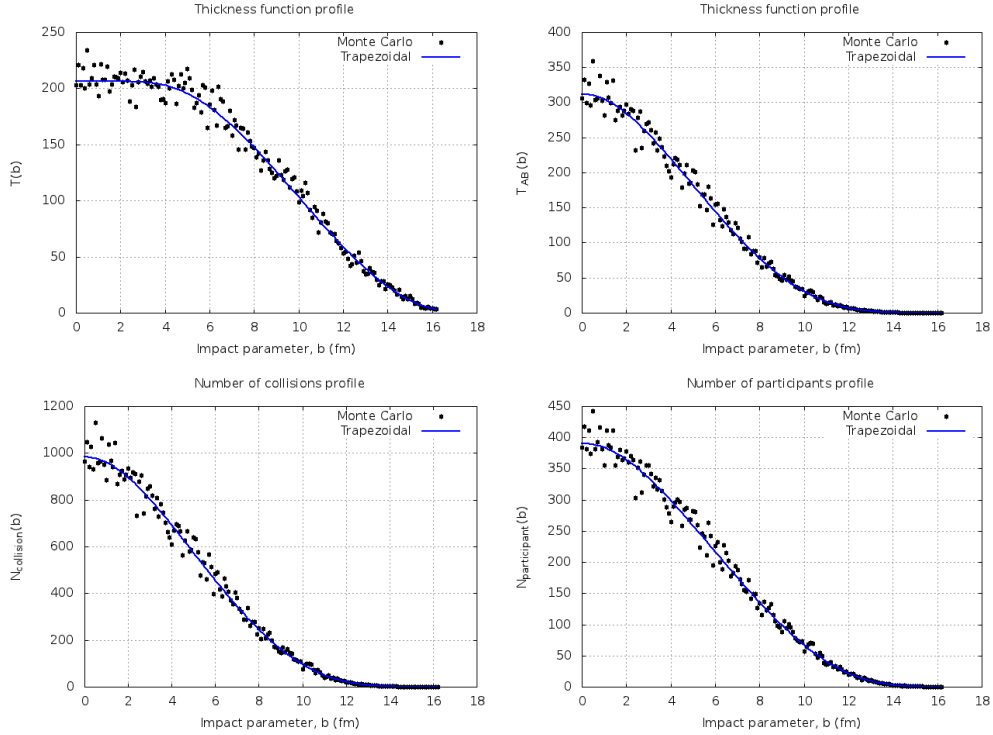


Figure 3.6: Comparison of results from different computation techniques

We find excellent agreement between the two techniques used.

Though the optical form of Glauber model gives us reasonable insight into the role of geometrical considerations and its implications in nucleus – nucleus collision based experiments, the theory rests on continuous nucleon density distribution. It fails to locate the nucleons at specific spatial coordinates. In order to account for the discreteness of the nucleus, Monte Carlo formulation of the Glauber model is used.

# Chapter 4

## Monte Carlo Glauber Model

In the Monte Carlo based Glauber model, the individual nucleons are randomly distributed event-by-event and collision properties are calculated by averaging over multiple events where an event refers to collision of two nuclei.

### 4.1 Coding the model

Given a large number of Monte Carlo events to be simulated in order to get the relationship between the number of participating nucleons and number of binary collisions with the impact parameter of the nucleus – nucleus collision, the following steps are taken.

1. An impact parameter for the collision is selected randomly from the distribution

$$\frac{dN}{db} \propto b$$

where  $N$  is the number of events and  $b$  is the impact parameter.

2. For each impact parameter, the nucleons in the nucleus are distributed in accordance with the given nuclear density distribution. The radial part of distribution is  $r^2 \rho(r)$ , where  $r$  is the radial distance of the nucleon from the center of the nucleus. The polar part is weighted by  $\sin(\theta)$ , where  $\theta$  is the polar angle of the nucleon and belongs to the range  $(0, \pi)$ . The azimuthal part is picked from uniform distribution from  $(0, 2\pi)$ . This is done as the elementary volume in spherical polar coordinate system is given by  $4\pi r^2 dr \sin(\theta) d\theta d\phi$ .

3. The centers of the two colliding nuclei are shifted to  $(-b/2, 0, 0)$  and  $(b/2, 0, 0)$  respectively.

4. Two nucleons from different nuclei are said to collide if the transverse distance between them,  $d$ , satisfies

$$d \leq \sqrt{\frac{\sigma_{inel}^{NN}}{\pi}}$$

5. For each event, the total number of binary collisions  $N_{coll}$  is calculated by the sum of individual number of collisions and the total number of participating nucleons,  $N_{part}$ , is the number of nucleons that interact only once.

The details are discussed in the appendix.

## 4.2 Results and Discussions

A typical Au+Au collision at 200 GeV from the Monte Carlo Glauber model appears as in Fig. 4.1 where the darker shades represent the participants while the lighter shades represent the spectators.

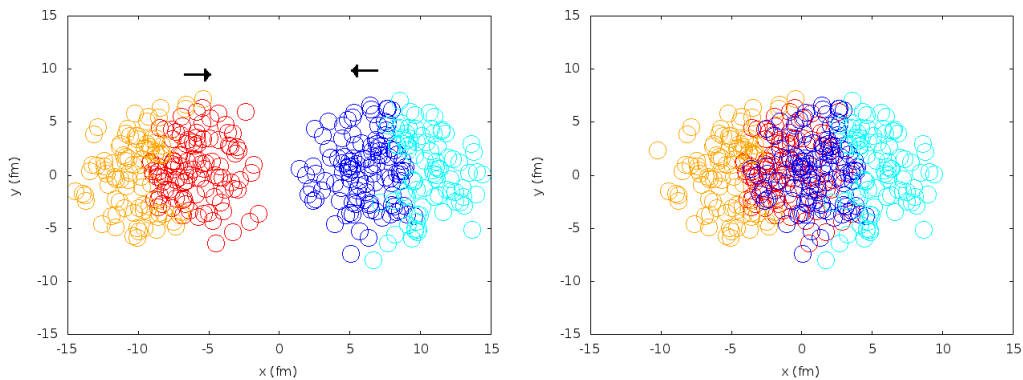


Figure 4.1: Typical Monte Carlo Event for Au+Au collisions at impact parameter of 6 fm. The red and blue circles are the participating nucleons, the diffused colored circles are spectator nucleons before (left) and after (right) collision.

In order to compare the results with its optical counterpart, Monte Carlo simulations are performed for Pb–Pb collision within the center of mass energy range of 7 to 60 GeV and  $\sigma_{inel}^{NN} = 31.5$  mb as in the previous case. The analysis of number of participants and the number of binary collisions is made for the Woods – Saxon form of the nuclear density profile as given in Table 3.1.

Comparison of results from the two formalisms is shown in Fig. 4.2.

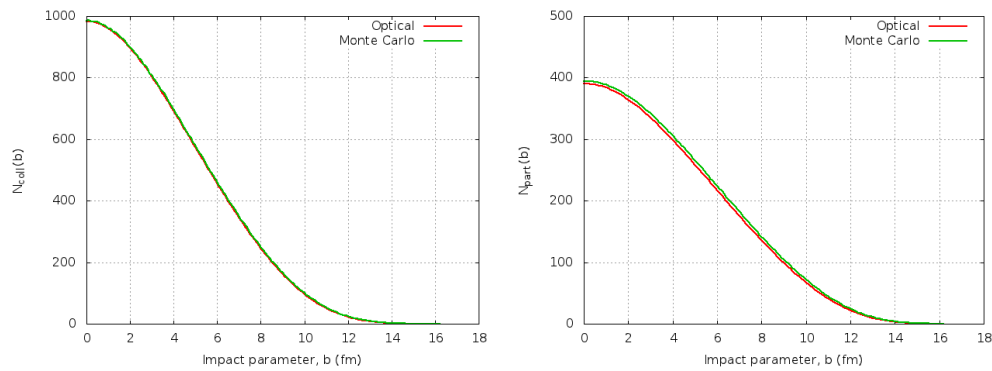


Figure 4.2: Comparison of results from Monte Carlo and Optical Glauber formalisms.

The optical limit assumes that the scattering amplitudes can be described using the approximation that the projectile nucleons see the target nucleons as a smooth density. This leads to slight distortions in the estimation of the number of participants and the number of binary collisions compared to the Monte Carlo approach. In addition, the local density fluctuations are considered event–by–event in the latter approach.

# Chapter 5

## Relating Glauber Model to experiments

As a matter of fact, neither number of participants nor the number of binary collisions can be directly measured in an experiment. Added to that, even the impact parameter cannot be determined directly. In order to understand the applicability of the Glauber model to experiments, we employ a mapping to the number of charged particles produced by defining centrality classes in both measured and calculated distributions. The basic assumption for defining the centrality classes is that the impact parameter  $b$  is monotonically related to particle multiplicity. For large  $b$  (peripheral) events, charged particle multiplicity is low at mid-rapidity and a large number of spectator nucleons are present, while for small  $b$  (central) events, multiplicity is high and number of spectators is low.

### 5.1 Production of charged particles

The charged particle multiplicity in  $pp$  collisions per unit rapidity has contributions due to two components – soft processes and hard processes. Soft processes are those which lead to production of low energy hadrons like pions in nucleus – nucleus collision. These cannot be described by perturbative QCD as the strong coupling constant is large. The appropriate scaling of multiplicity of soft processes is postulated to be the number of participating nucleons. This is because multiple soft collisions change only the excited states of the nucleons, which in turn produce particles the moment they leave the interaction region. The pions with large transverse momenta are pro-

duced by hard processes like jets. As the strong coupling constant is small for these processes, they can be described within the methods of perturbative QCD. For hard processes, the number of particles produced is assumed to scale with the number of binary collisions.

Assuming  $x$  as the fraction of charged particle multiplicity,  $n_{pp}$  measured in  $pp$  collisions per unit pseudo-rapidity due to hard processes and the remaining  $(1 - x)$  due to soft processes [13],

$$\frac{dN_{ch}}{d\eta} = n_{pp} \left[ (1 - x) \frac{N_{part}}{2} + x N_{coll} \right] \quad (5.1)$$

The factor 0.5 associated with number of participating nucleons is to consider particle produced per participating nucleon pair. This compares well with the experimental data [24] as shown in Fig. 5.1 with the value of  $x$  to be  $0.11 \pm 0.02$  for  $\sqrt{s_{NN}} = 200$  GeV.

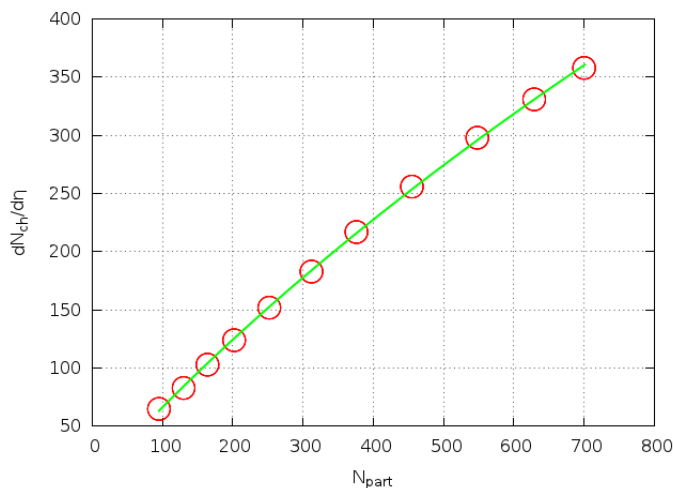


Figure 5.1: The measured pseudorapidity density of charged particles  $dN_{ch}/d\eta$  for  $|\eta| \leq 1$  as a function of  $N_{part}$  for Au+Au collisions at  $\sqrt{s_{NN}} = 200$  GeV. The solid line is the two component model (Equation 5.1) fit to the data.

Event – by – event multiplicity fluctuations can be taken into account by convo-

luting Negative Binomial Distribution (NBD) for a given  $N_{part}$  and  $N_{coll}$

$$P(\mu, k; n) = \frac{\Gamma(n+k)}{\Gamma(n+1)\Gamma(k)} \left(\frac{\mu}{k}\right)^n \left(1 + \frac{\mu}{k}\right)^{-(n+k)} \quad (5.2)$$

where  $\mu$  is the mean of the distribution and  $k$  is a second parameter affecting the width of the distribution.  $\mu$  and  $k$  are related to  $N_{part}$  and  $N_{coll}$  as :

$$\mu = \alpha \left[ (1-x) \frac{N_{part}}{2} + x N_{coll} \right] \quad k = \beta \left[ (1-x) \frac{N_{part}}{2} + x N_{coll} \right] \quad (5.3)$$

The parameter  $\alpha$ ,  $\beta$  and  $x$  are obtained by fitting the experimental data and using  $\chi^2$  - optimization.

The NBD has two parameters,  $\mu$  and  $k$ . The parameter  $k$  is an interesting quantity,  $1/k \rightarrow 0$  would correspond to Poisson distribution (independent particle production) and  $k = 1$  would correspond to geometric distribution. Under the limit of large multiplicity ( $n \rightarrow$  large), the NBD distribution goes over to a gamma distribution. Some of the measured multiplicity distributions at midrapidity ( $|\eta| \leq 0.5$ ) are fitted to NBD distribution [15] as shown in Fig. 5.2.

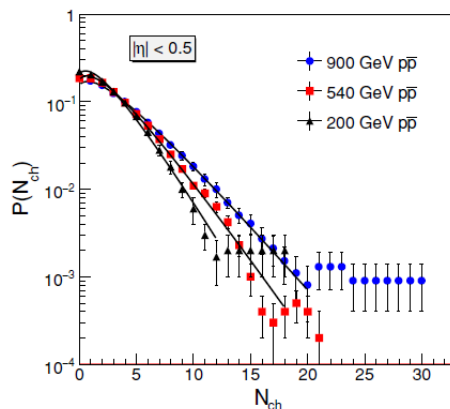


Figure 5.2: Multiplicity distribution for charged particles in  $p + \bar{p}$  collisions at various center of mass energies at midrapidity. The solid lines are Negative Binomial Distribution fit to the data.

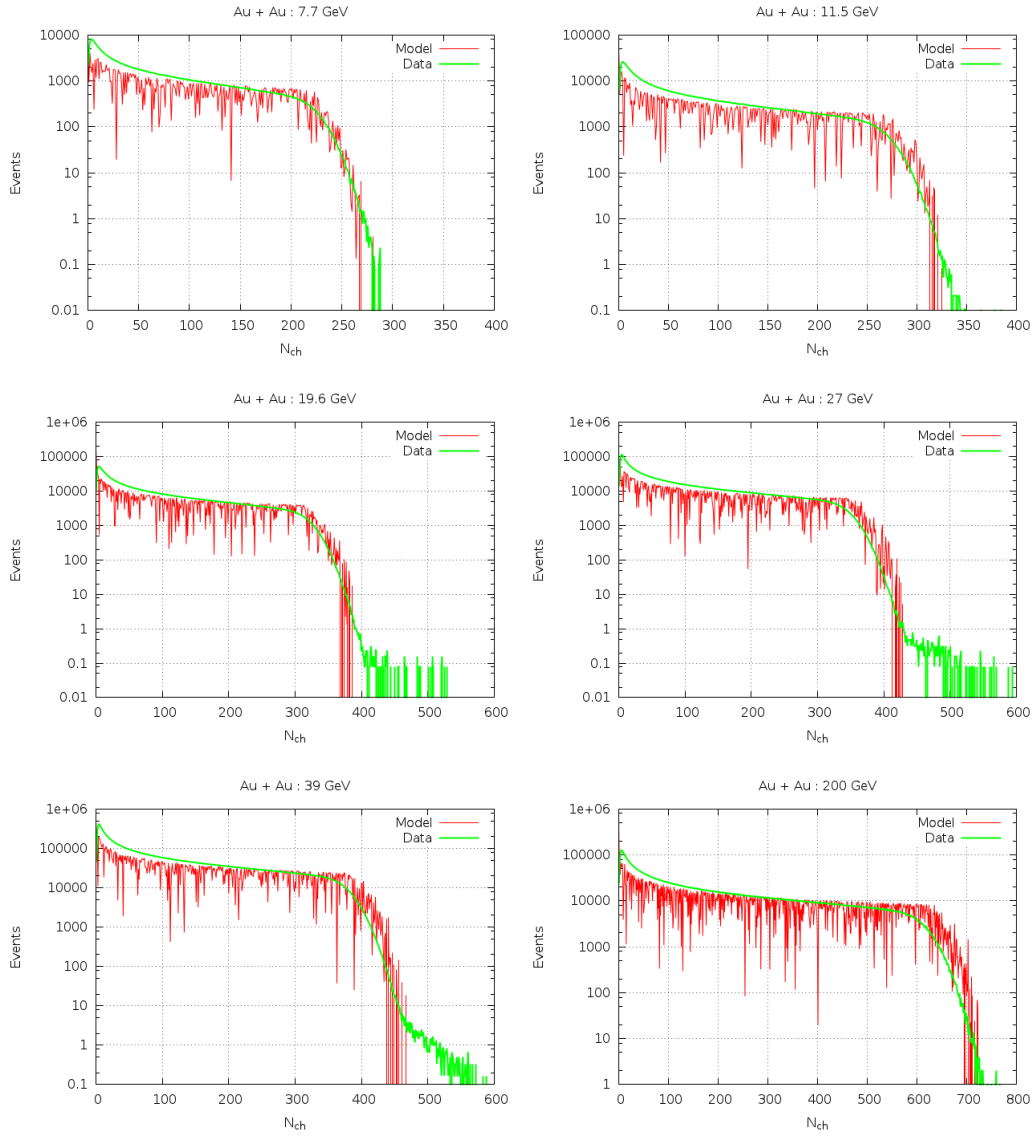


Figure 5.3: Charged particle multiplicity distribution for Au + Au collision at various energies.

The experimental data for charged particle multiplicity for energy ranging from 7.7 GeV to 200 GeV for Au + Au collision at RHIC is fitted to the model (Fig. 5.3) by optimizing the values of  $x$ ,  $\alpha$  and  $\beta$ . The values are tabulated in Table 5.1.

Table 5.1: Values of charged particle multiplicity parameters fit to data

$\sqrt{s}$ (GeV)	$x$	$\alpha$	$\beta$
7.7	0.12	0.89	2
11.5	0.12	1.07	2
19.6	0.12	1.27	1.8
27	0.12	1.385	1.65
39	0.12	1.49	2
200	0.13	2.38	1.95

We find that using the three parameter two-component model, we are able to explain the charged particle multiplicity as seen in experiments to a large extent.

## 5.2 Eccentricity

The system of heavy ion collision is surrounded by vacuum. This gives rise to a pressure gradient from the dense center to the boundary of the system. This pressure gradient is radially symmetric for central heavy ion collisions and gives a radially outward boost to all particles that are formed in the system. This influences the transverse momentum spectra of heavy particles. For non – central collisions, the shape of the interaction region depends strongly on the impact parameter of the collision. Just after the collision, as shown in Fig. 5.4, the reaction volume is elliptically shaped. This spatial anisotropy with respect to the  $x - z$  plane translates into the momentum anisotropy of the produced particles.

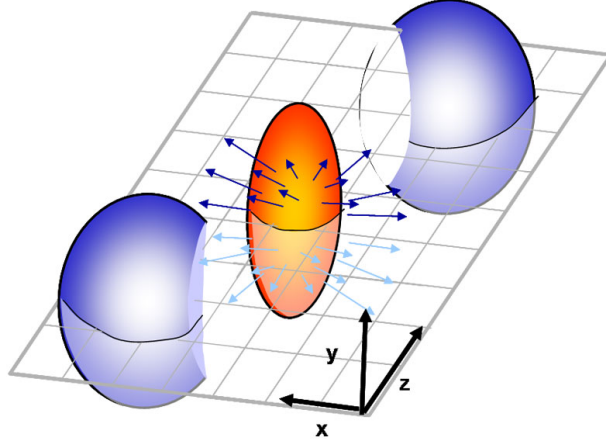


Figure 5.4: Non-central nucleus – nucleus collision.

The initial space anisotropy, characterized by the eccentricity [16], is defined as

$$\epsilon_{RP} = \frac{\sigma_y^2 - \sigma_x^2}{\sigma_y^2 + \sigma_x^2} \quad (5.4)$$

$$\epsilon_{PP} = \sqrt{\frac{(\sigma_y^2 - \sigma_x^2)^2 + 4\sigma_{xy}^2}{\sigma_y^2 + \sigma_x^2}} \quad (5.5)$$

where  $\sigma_x^2 = \langle x^2 \rangle - \langle x \rangle^2$ ,  $\sigma_y^2 = \langle y^2 \rangle - \langle y \rangle^2$  and  $\sigma_{xy}^2 = \langle xy \rangle - \langle x \rangle \langle y \rangle$ .  $RP$  stands for reaction plane and  $PP$  for the participant plane. For participant plane calculations, the coordinated axes are aligned in the direction of the major and minor axes of the ellipse formed in the collision region as shown in Fig. 5.5.

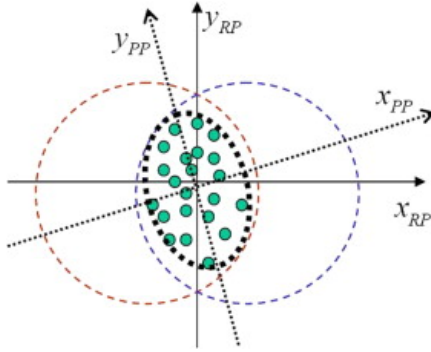


Figure 5.5: Reaction plane and participant plane.

The variation of eccentricity with impact parameter is shown in Fig. 5.6. One notices that the standard eccentricity goes to zero for collisions with zero impact parameter, as one would expect for two spherical shaped objects. But for participant eccentricity one finds it still has some non-zero value for zero impact parameter collisions. This is because it is calculated considering the distribution of nucleons inside the nuclei.

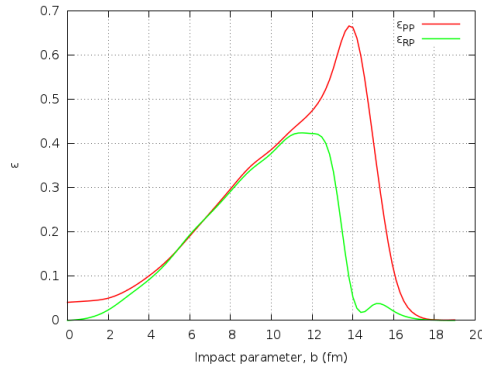


Figure 5.6: Variation of eccentricity with impact parameter.

With increase in the collision energy, eccentricity decreases (Fig. 5.7). If the eccentricity is participant eccentricity, it would depend on the number of participating nucleons and hence their positions. This number changes with energy, so one may expect participant eccentricity also to change.

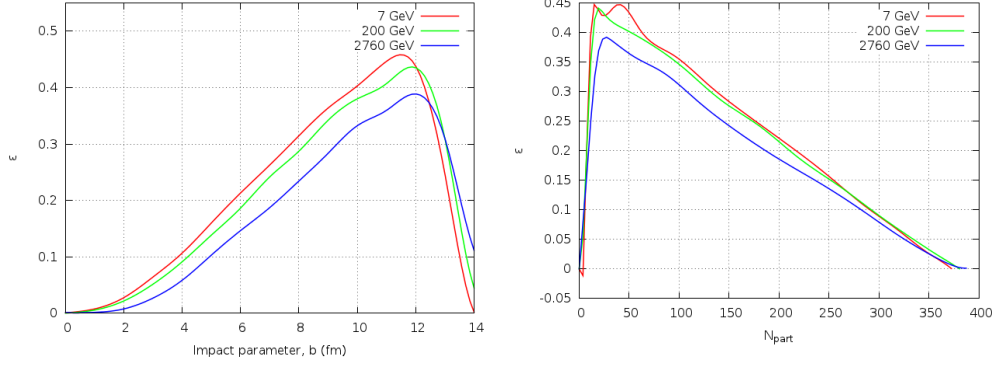


Figure 5.7: Variation of eccentricity for different energies with impact parameter(left) and  $N_{part}$  (right) for Au + Au collision.

As already discussed, the initial spatial anisotropy results in anisotropy in the momentum of the produced particles. A measure of this momentum anisotropy is  $v_2$  given by

$$v_2 = \left\langle \frac{p_x^2 - p_y^2}{p_x^2 + p_y^2} \right\rangle \quad (5.6)$$

According to ideal hydrodynamics [17], elliptic flow ( $v_2$ ) is proportional to initial spatial eccentricity.

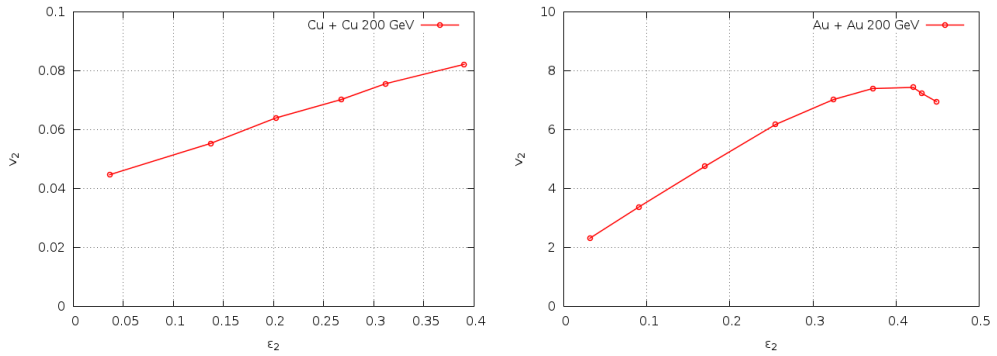


Figure 5.8: Relation between elliptic flow and initial spatial eccentricity for Cu + Cu (left) and Au + Au (right) at 200 GeV.

In Fig. 5.8, we have plotted the  $v_2$  (momentum space anisotropy measured in

experiments) versus the spatial anisotropy obtained for the same centrality as the experimental data using Glauber model. The figure clearly depicts this transformation from spatial anisotropy to momentum anisotropy for the system formed in the heavy-ion collisions. The slope of the curve decides how efficient is this transformation. There could be several physical effects which can dampen this transformation, one such effect is viscosity.

### 5.3 Angular momentum

Nuclei colliding at ultra-relativistic energies, in principle, should carry large initial angular momentum if the impact parameter is non-zero because of the homogeneity of the colliding nuclei in the transverse plane. From angular momentum conservation in peripheral ultra-relativistic heavy ion collision, this large initial angular momentum must be transferred to the initial angular momentum of the quark – gluon plasma, leading to enhanced azimuthal anisotropy of particle spectra. In hydrodynamical terms, the initial angular momentum has a non-trivial dependence on the initial longitudinal flow velocity on the transverse co-ordinates, thereby giving rise to non-vanishing vorticity in the equations of motion [18]. This enhances the expansion rate of the supposedly created fluid and also compensates for the possible effect of viscosity. The most distinctive signature of the vorticity in the plasma would be the average polarization of the emitted hadrons. Here we provide an estimate of the initial angular momentum generated by the system of colliding ions at relativistic energies

The angular momentum  $\vec{L}$  is given by

$$\vec{L} = \vec{r} \times \vec{p} \tag{5.7}$$

In the case of ultra-relativistic collisions, we can take  $r^2 = x^2 + y^2$  where we consider the beam to be moving in  $z$ -direction. The linear momentum is along the

beam direction and hence  $\vec{p} = p_z \hat{z}$  for the projectile nucleus and  $\vec{p} = -p_z \hat{z}$  for the target nucleus. From this we get that

$$\vec{L} = rp_z \hat{y} \quad (5.8)$$

Angular momentum of participating nucleons from nucleus moving in +z direction is taken to be negative while those from that moving in -z direction is taken to be positive. The outline of the program used to compute the variation of angular momentum with impact parameter is given in the appendix.

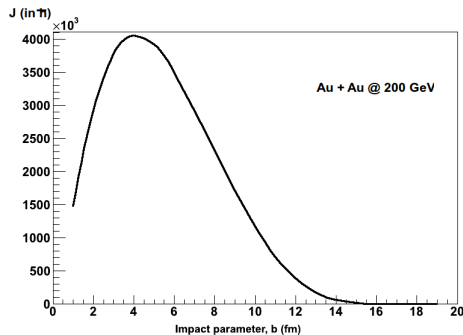


Figure 5.9: Variation of angular momentum with impact parameter for Au + Au collision at  $\sqrt{s_{NN}} = 200$  GeV.

As compared to the angular momentum of the electron in hydrogen atom, this is more than two million times larger. For two colliding gold nuclei, the value of the initial angular momentum of the interaction region was found to be very large and also to have a strong dependence on the impact parameter (Fig. 5.9).

## 5.4 Electromagnetic field

Nucleus – nucleus collisions address the possibility for nuclear matter to undergo phase transitions into a new state of matter. As the motion of two fast moving nuclei in off-central heavy ion collision is oppositely directed, strong transient electromag-

netic fields can be created. The order of magnitude can be as high as  $10^{15}$  Tesla for magnetic field in the direction of the angular momentum. Such high magnetic fields can convert topological charge fluctuation in QCD vacuum into global electric charge separation with respect to the reaction plane as preferential emission of charged particles occurs along the direction of angular momentum due to presence of non-zero chirality. This is the chiral magnetic effect [19]. Besides this, other effects like catalysis of chiral symmetry breaking, the possibility of chiral and deconfinement phase transitions, the spontaneous electromagnetic superconductivity of QCD vacuum, the possible enhancement of elliptic flow of charged particles etc. are also caused by strong magnetic fields.

Using the Liènard – Weichert potentials to calculate the electric and magnetic fields at position  $\mathbf{r}$  and time  $t$  [20],

$$e\vec{E}(t, \vec{x}) = \alpha_{EM} \sum_{n=1}^{N_{part}} \frac{1 - v_n^2}{R_n^3 \left(1 - \left[\vec{R}_n \times \vec{v}_n\right]^2 / R_n^2\right)^{3/2}} \vec{R}_n |_{t_r} \quad (5.9)$$

$$e\vec{B}(t, \vec{x}) = \alpha_{EM} \sum_{n=1}^{N_{part}} \frac{1 - v_n^2}{R_n^3 \left(1 - \left[\vec{R}_n \times \vec{v}_n\right]^2 / R_n^2\right)^{3/2}} \vec{v}_n \times \vec{R}_n |_{t_r} \quad (5.10)$$

where  $\alpha_{EM}$  is the fine structure constant and  $\vec{R}_n = \vec{x} - \vec{x}_n(t)$  where  $\vec{x}_n$  is the position of proton moving with velocity  $\vec{v}_n$  and  $t_r$  is the retarded time. If  $\vec{v}_n = v\hat{z}$ , then  $\left[\vec{R}_n \times \vec{v}_n\right]^2 = R_{n,\perp}^2 v_n^2$  where  $R_{n,\perp}$  is time – independent.

At  $t = 0$ , the proton positions are distributed in accordance with the Woods – Saxon distribution. We assume that all the target nucleons move with  $\vec{v}_n^{targ} = (0, 0, v)$  and the projectile nucleons with  $\vec{v}_n^{proj} = (0, 0, -v)$ . If the collision energy is  $\sqrt{s}$  and mass of proton is  $m_p$  then

$$v^2 = 1 - \left(\frac{2m_p}{\sqrt{s}}\right)^2 \quad (5.11)$$

A cut off of  $r_{cut} = 0.3$  fm as an effective distance between two nucleons is implemented to take care of the singularity at  $R_n \rightarrow 0$ . A very weak dependence of the electric and magnetic fields were observed on  $r_{cut}$  in the range of 0.3 fm to 0.6 fm.

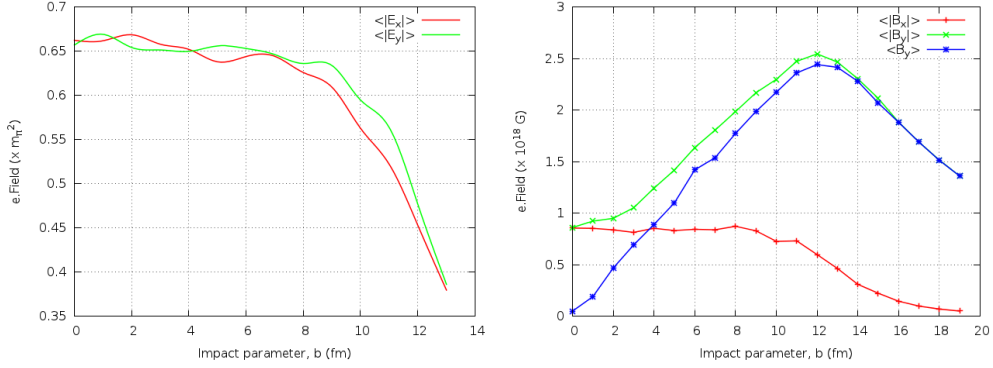


Figure 5.10: Event – by – event variation of electric field (left) and magnetic field (right) with impact parameter for Au + Au collision at  $\sqrt{s_{NN}} = 200$  GeV.

The Fig. 5.10 shows the variation of electric and magnetic field for different impact parameters. Due to the symmetry of the system about the  $y$ -axis,  $\langle E_x \rangle = \langle E_y \rangle = \langle B_x \rangle = 0$ . These are non-zero on an event-by-event basis. With increase in collision energy, the magnitude of magnetic field increases drastically, as shown in Fig. 5.11.

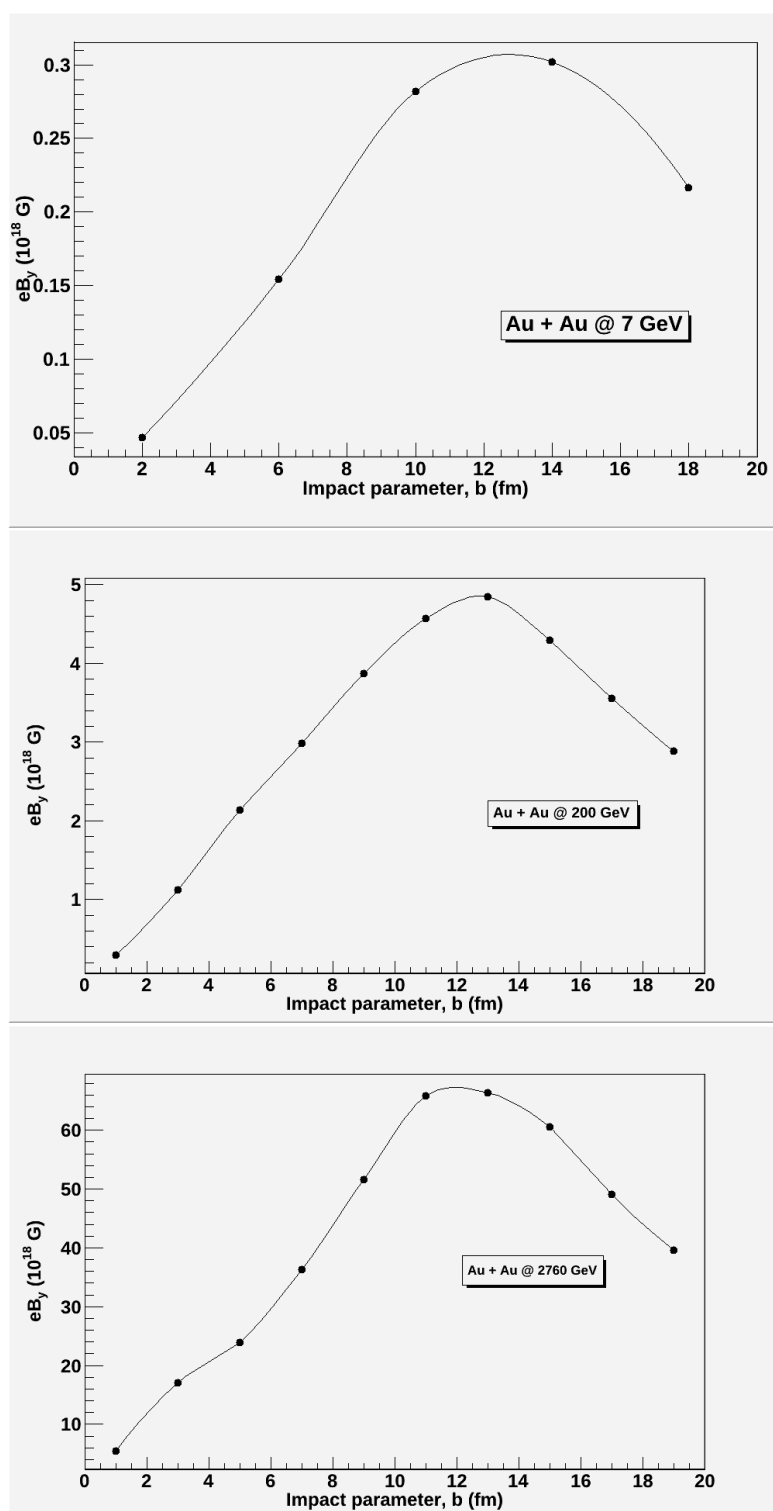


Figure 5.11: Event – by – event variation of magnetic field with impact parameter for different values of beam energies for Au + Au collision.

We find that huge transient magnetic field of the order of  $10^{18}$  G is produced as compared to typical values of 0.5 G for earth's magnetic field,  $10^7$  G for the strongest man-made magnetic field and  $10^{16}$  G on the surface of magnetostars. These are transient fields which act on time-scales of the order of a few fm/c (Fig. 5.12). But this is enough for its effect to be encoded as the lifetime of the Quark – Gluon Plasma is predicted to be around 6 – 10 fm/c.

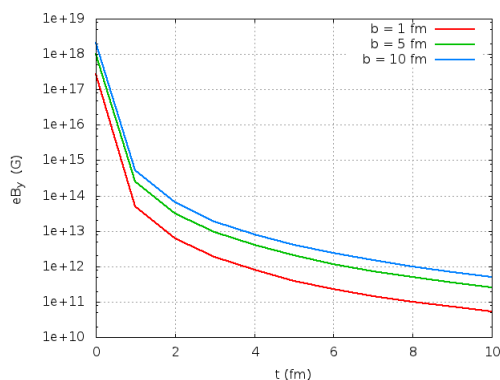


Figure 5.12: Time evolution of magnetic field

# Chapter 6

## Multiplicity fluctuations from Glauber Model

At present, a lot of theoretical and experimental investigations of multiplicity and transverse momentum fluctuations of charged particles in high energy heavy ion collisions is carried out. This is because we expect an increase in fluctuations in the case of freeze-out close to the critical endpoint of QCD and at the hadronic matter phase boundary separating the QGP [23]. But there may be other factors which lead to an increase in fluctuations and need to be eliminated. Fluctuations in the number of participants and binary collision lead to fluctuations in the number of particle sources which directly lead to fluctuations in multiplicity and transverse momentum of the produced charged particles. Other sources of fluctuations can be listed as follows :

1. finite charged particle multiplicity
2. effect of limited acceptance of the detector
3. impact parameter fluctuations
4. effect of rescattering due to secondary collisions

In this report, we will be discussing the effect of fluctuations in number of participants on fluctuations in the number of charged particles produced as derived from Monte Carlo Glauber model.

The relative fluctuation of a parameter  $X$  is given by

$$\omega_X = \frac{\sigma_X^2}{\langle X \rangle} \quad (6.1)$$

where  $\sigma_X^2 = \langle X^2 \rangle - \langle X \rangle^2$ .

From a simple participant model, the charged particle multiplicity is expressed as

$$N = \sum_{i=1}^{N_{part}} n_i \quad (6.2)$$

where  $N_{part}$  is the number of participants and  $n_i$  is the number of particles produced in the detector acceptance by the  $i^{th}$  participant. On an average, the mean value of  $n_i$  is the ratio of the average multiplicity in the detector coverage to the average number of participants, hence

$$\langle n \rangle = \langle N \rangle / \langle N_{part} \rangle \quad (6.3)$$

Thus, the fluctuations in  $N$  will have contributions due to fluctuations in  $N_{part}$  ( $\omega_{N_{part}}$ ) and also due to the fluctuations in the number particles produced per participant ( $\omega_n$ ). In the absence of correlations between the  $n_i$ , the multiplicity fluctuations  $\omega_N$  is expressed as

$$\omega_N = \omega_n + \langle n \rangle \omega_{N_{part}} \quad (6.4)$$

The participant model is expected to hold reasonably well for peripheral collisions where there are only few nucleon – nucleon collisions, while for central collisions the particle production gets affected by nucleon – nucleon scattering, rescatterings between produced particles, energy degradation, and other effects.

The effect of fluctuation in impact parameter can be captured in the fluctuation in number of participants which is be obtained from Monte Carlo Glauber calculations. The quantity  $\langle n \rangle$  is equal to the ratio of the mean charged particle multiplicity for a given acceptance to the mean number of participants for the same centrality bin. The mean charged particle multiplicity is obtained by using the two–component charged particle multiplicity relation as given in Eq. 5.1.  $\langle m \rangle$  is the total number of particles produced per participant and from literature [24]

$$\langle m \rangle = \langle N_{ch} \rangle^{NN} = -4.7 + 5.2s^{0.145} \quad (6.5)$$

for  $\sqrt{s}$  between 2 to 500 GeV. This is used to calculate  $\omega_m$  which is given by

$$\omega_m = 0.33 \frac{(\langle N_{ch} \rangle - 1)^2}{\langle N_{ch} \rangle} \quad (6.6)$$

Fluctuation in  $n$  will then be given according to

$$\omega_n = 1 - \frac{\langle n \rangle}{\langle m \rangle} + \frac{\langle n \rangle}{\langle m \rangle} \omega_m \quad (6.7)$$

Hence we can compute the fluctuations in number of participants and charged particle multiplicity.

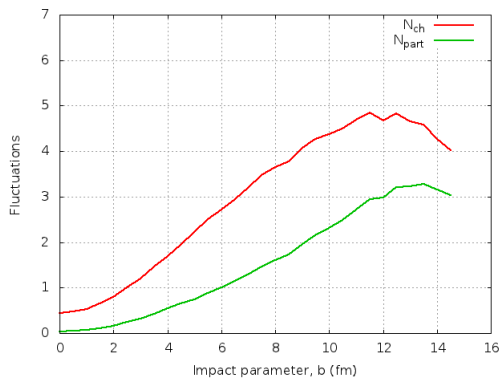


Figure 6.1: Variation of fluctuations with impact parameter

From Fig. 6.1, we conclude that a large contribution to charged particle multiplicity comes from the fluctuation in the number of participants and this needs to be taken into account and eliminated carefully when studying fluctuations due to critical behavior in the evolution of system.

# Chapter 7

## Summary and Conclusions

The Glauber model provides a quantitative consideration of the geometrical configuration of the nuclei when they collide. It treats the nucleus-nucleus collision as a series of nucleon-nucleon collision process. In order to compare the geometric results of this model with real experimental data the nuclear density profile and the inelastic nucleon-nucleon cross-section is given as model inputs. The static cross-section is assumed to be the same as that for proton proton collision and does not depend on the nuclear environment. This is the only non-trivial dependence of the model on the beam energy.

The Glauber model provides us with the number of participating nucleons and the number of binary collisions for a given impact parameter at a given center of mass energy. The model comes in two variants namely the Optical Glauber model and the Monte Carlo Glauber model. While in Optical Glauber model the nucleus is considered as a smooth matter density, in the Monte Carlo variant, the nucleons in the nucleus are populated stochastically according to the given nuclear density profile. For the Optical Glauber model, the number of binary collisions and participating nucleons are derived analytically; in the Monte Carlo version, it is counted.

In order to understand the applicability of the Glauber model, we map it to the number of charged particles produced by defining centrality classes. We can see that a simple geometrical model explains the charged particle multiplicity data obtained for energies ranging from 7 GeV to 200 GeV gold on gold collision at RHIC for  $|\eta| \leq 0.5$ .

Just after collision, for a non-central collision, the reaction volume is elliptically

shaped. The pressure gradient is more towards the center and lesser towards the ends. This initial spatial anisotropy is characterized by eccentricity and translates to momentum anisotropy of produced particles. From experiments, we find that this momentum anisotropy given by  $v_2$  is proportional to eccentricity. From this simple geometric model, we can calculate eccentricity and establish the anisotropy in momentum space as a consequence of anisotropy of collision geometry.

Due to inhomogeneity in the colliding nuclei in the transverse plane, from Glauber model calculations we find that these systems carry very large angular momentum. From conservation of angular momentum, this must be transferred to the initial angular momentum of the quark gluon plasma. This uncompensated angular momentum may affect the initial longitudinal flow velocity. We still need a sound theoretical calculation which includes the effect of large initial angular momentum.

Heavy nuclei are huge bunches of charges moving at relativistic speeds. We find that huge transient magnetic field of the order of  $10^{18}$  G is produced. Such high magnetic fields lead to novel effects like chiral magnetic effect signatures of which are observed in RHIC. These transient fields act on time scales of few fm/c. But this is enough for its effects to be encoded as the lifetime of quark gluon plasma is predicted to be around 5 fm/c. Thus we see how simple geometrical considerations can lead to explanation of results in high energy heavy ion collision.

Fluctuations have gained importance with the increasing search for the critical point at RHIC. But fluctuations in the number of participants, binary collision and number of charged particles produced should be taken into account and eliminated accordingly when looking for the critical point. From this very simplistic geometrical model, we can provide a baseline over which effects of fluctuations start gaining importance.

To conclude, the Glauber model, though very simplistic, is able to explain diverse

effects as seen in high energy heavy ion collisions only based on geometric considerations.

# References

- [1] Ultra-relativistic Heavy Ion Collision by Romana Vogt, Elsevier, 2007.
- [2] Introduction to High Energy Heavy Ion Collisions by C. Y. Wong, World Scientific, Singapore, 1994
- [3] P. Shukla, arXiv : nucl-th/0112039v1.
- [4] M. L. Miller et al, arXiv : nucl-ex/0701025v1.
- [5] WA98 Collaboration, arXiv : nucl-ex/0008004v2
- [6] R. Haque et al, Phys. Rev. C 85 034905 (2012)
- [7] S. S. Alder et al, Phys. Rev. Lett. 91 241803 (2003)
- [8] J. Adams et al, Phys. Lett. B 637 (2006) 161.
- [9] Particle Data Group.
- [10] B. Schenke et al, arXiv : hep-ph/1206.6805v1
- [11] A. Bzdak, arXiv : hep-ph/0807.1389v1
- [12] B. Alver et al, arXiv : nucl-ex/0805.4411v1
- [13] D. Kharzeev et al, Phys. Lett. B 507 (2001) 121 – 128
- [14] PHOBOS Collaboration arXiv : nucl-ex/0201005v2
- [15] A. K. Dash et al, J. Phys. G 37 025102 (2010)
- [16] H. Masui et al, arXiv : nucl-th/0907.0202v2

- [17] R. Snellings, arXiv : nucl-ex/1102.3010v2
- [18] F. Becattini et al, Phys. Rev. C 77 024906 (2008)
- [19] H. J. Warringa, arXiv : hep-ph/0906.2803v1
- [20] A. Bzdak et al, arXiv : hep-ph/1111/1949v2
- [21] V. V. Skokov et al, arXiv : nucl-th/0907.1396v1
- [22] W. T. Deng et al, arXiv : nucl-th/1201.5108v2
- [23] V. V. Vechernin et al, arXiv : hep-ph/1102.2582v2
- [24] M. M. Agrawal et al, Phys. Rev. C 65 054912 (2002)

# Appendix A

## Numerical integration techniques

### 7.1 Trapezoidal integration

The trapezoidal rule is a technique of numerical integration which works by approximating the region under the graph of a function  $f(x)$  as series of trapezoids and calculating its area.

$$\int_a^b f(x) dx \approx (b-a) \frac{f(a) + f(b)}{2}. \quad (7.1)$$

In order to carry out trapezoidal integration, we divide the region of integration into  $n$  bins, each of whose width is given by

$$h = \frac{b-a}{n}$$

Hence we have,

$$\int_a^b f(x) dx = h \times \left[ \frac{f(a) + f(b)}{2} + \sum_{i=1}^{n-1} f(a+ih) \right] \quad (7.2)$$

For two dimensional integration, we define

$$h = \frac{b-a}{m} \quad k = \frac{d-c}{n}$$

and

$$x_i = a + ih \quad i = 0, 1, \dots, m$$

$$y_i = c + ik \quad i = 0, 1, \dots, n$$

Hence we get,

$$\begin{aligned}
 \int_c^d \int_a^b f(x, y) dx dy &= \frac{hk}{4} [f(a, c) + f(a, d) + f(b, c) + f(b, d)] \quad (7.3) \\
 &+ 2 \sum_{i=1}^{m-1} f(x_i, c) + 2 \sum_{i=1}^{m-1} f(x_i, d) \\
 &+ 2 \sum_{i=1}^{n-1} f(a, y_i) + 2 \sum_{i=1}^{n-1} f(b, y_i) \\
 &+ \sum_{i=1}^{m-1} \sum_{y=1}^{n-1} f(x_i, y_j)
 \end{aligned}$$

## 7.2 Monte Carlo integration

Monte Carlo integration is an integration technique which is based on a sequence of random numbers. If we are interested in computing an integral  $\int_a^b dx f(x)$ . We do a linear transformation on so that we get a sequence of random numbers  $x_i$  which are uniformly distributed between  $[a, b]$ . The transformation is

$$x(y) = (b - a)y + a$$

where  $y \in U [0, 1]$  If the sequence of random numbers consists of  $N$  values of  $x_i$ , an estimate of the integral is

$$\int_a^b dx f(x) = \frac{b - a}{N} \sum_{i=1}^N f(x_i) \quad (7.4)$$

The estimate on the right is the Monte Carlo estimate and the estimates improves as one chooses larger value of  $N$ .

When the region of multi-dimensional integration is regular, the generalization of Monte Carlo method is trivial. A two dimensional integral reduces to

$$\int_a^b dx \int_c^d dy f(x, y) = \sum_{i=1}^N \frac{(d - c)(b - a)}{N} f(x_i, y_i) \quad (7.5)$$

where the region of integration is a rectangle. For faster estimates, we can employ the techniques of importance sampling in order to choose our random points for integration.

# Appendix B

## Computing angular momentum

The main part of the C++ code used to compute the angular momentum is as follows :

1. The collision parameters like the mass number, atomic number and nuclear density profile function of the colliding nucleons, energy of collision, and inelastic nucleon – nucleon cross–section is obtained from the user.
2. According to the given nuclear density profile function, the positions of the nucleons are assigned taking into consideration the impact parameter for collision.
3. The participant positions are determined using Monte Carlo Glauber model approach.
4. In order to get the angular momentum,  $L$ , the transverse distance  $r = \sqrt{x^2 + y^2}$  is calculated for the participating nucleon and is multiplied with the longitudinal momentum.
5. For nucleons of nucleus A whose center is shifted to  $(b/2)$ ,  $L$  is replaced by  $-L$  if the  $x$ -coordinate is negative. This was done to ensure that nucleons of nucleus A have positive angular momentum. Similar steps are used to make sure that nucleons of nucleus B have negative angular momentum as both are moving in opposite direction.
6. The net angular momentum is obtained by summing over angular momentum of all the participating nucleons.

# Appendix C

## Computing magnetic field

The main part of the C++ code used to compute the magnetic field is as follows :

1. The collision parameters like the mass number, atomic number and nuclear density profile function of the colliding nucleons, energy of collision, and inelastic nucleon – nucleon cross–section is obtained from the user.
2. According to the given nuclear density profile function, the positions of the nucleons are assigned taking into consideration the impact parameter for collision. The first A nucleons are labeled as protons for both the nuclei separately.
3. The spectator positions are determined using Monte Carlo Glauber model approach.
4. In order to get the magnetic field, the Liènard – Weichert potentials are used.

$$e\vec{B}(t, \vec{x}) = \alpha_{EM} \sum_n \frac{1 - v_n^2}{R_n^3 \left(1 - \left[\vec{R}_n \times \vec{v}_n\right]^2 / R_n^2\right)^{3/2}} \vec{v}_n \times \vec{R}_n \Big|_{t_r} \quad (7.1)$$

where  $\alpha_{EM}$  is the fine structure constant and  $\vec{R}_n = \vec{x} - \vec{x}_n(t)$  where  $\vec{x}_n$  is the position of proton moving with velocity  $\vec{v}_n$  and  $t_r$  is the retarded time. If  $\vec{v}_n = v\hat{z}$ , then  $\left[\vec{R}_n \times \vec{v}_n\right]^2 = R_{n,\perp}^2 v_n^2$  where  $R_{n,\perp}$  is time – independent. The retarded time is incorporated by employing Lorentz contraction in  $z$ -direction.

5. At  $t = 0$ , the proton positions are distributed in accordance with the Woods – Saxon distribution. We assume that all the target move with  $\vec{v}_n^{targ} = (0, 0, v)$  and  $\vec{v}_n^{proj} = (0, 0, -v)$ .

6. The net magnetic is obtained by summing over magnetic field produced by all the spectator nucleons.

# Appendix D

## Terminologies

- **Event** : It refers to the collision of two nuclei.
- **Multiplicity** : It is the total number of particles measured in the detectors after a heavy-ion collision.
- **Centrality** : Theoretically, centrality is characterized by the impact parameter which is the distance between the centers of two colliding heavy ions in a plane transverse to the beam direction. Small impact parameter collisions are central collisions while large impact parameter collisions are peripheral collisions. Experimentally, the collision centrality is inferred from the measured particle multiplicities if it is assumed that this multiplicity is a monotonic function of impact parameter. When the total integral of the multiplicity distribution is known, centrality classes are defined by binning the distribution based upon the fraction of the total integral.
- **Rapidity** : It is a dimensionless quantity defines in terms of the energy – momentum components of the particle and is related to the ratio of forward – to – backward light cone momentum. It is given by

$$y = \frac{1}{2} \ln \left( \frac{E + p_z}{E - p_z} \right)$$

- **Pseudo-rapidity** : It is a measure of the spatial coordinate describing the angle of a particle relative to the beam axis and is defined as

$$\eta = -\ln \left[ \tan \left( \frac{\theta}{2} \right) \right]$$

where  $\theta$  is the angle between particle momentum and beam axis.

- **Chirality** : For massless particles, chirality is the handedness of the particle. The chirality of a particle is right-handed if the direction of its spin is the same as the direction of its motion. It is left-handed if the directions of spin and motion are opposite. For massive particles, chirality is determined by whether the particle transforms in a right or left-handed representation of the Poincaré group.